01,07

Control of dilation anisotropy in the martensitic transformation region in the Ni-Mn-Ga-Si alloy

© I.I. Musabirov

Institute of Metal Superplasticity Problems, Russian Academy of Sciences,
Ufa, Bashkortostan, Russia

E-mail: irekmusabirov@mail.ru

Received October 15, 2025
Revised October 29, 2025
Accepted October 30, 2025

Martensitic transformation in Heusler alloys can be accompanied by various functional effects promising for practical application. However, this is hampered by high thermocycle brittleness in the as-cast state. This paper presents the results of a comparison of the dilation properties in the martensitic transformation region of a Ni-Mn-Ga-Si alloy in a coarse-grained state and with a bimodal structure possessing reduced thermocycle brittleness. It is shown that the formation of a bimodal structure by hot forging (700 °C, e = 3.2) results in the development of internal stresses (microstresses) of a preferred orientation, leading to the formation of martensite twins' transverse to the compression axis of the final forging stage. A rod-shaped specimen cut along this direction is abruptly compressed, while one cut across it, on the contrary, is elongated during the direct martensitic transformation. Thus, using hot forging it is possible to control the dilation anisotropy in the process of martensitic transformation of the Heusler Ni-Mn-Ga.

Keywords: Ni-Mn-Ga alloy, Heusler alloy, martensitic transformation, dilation, microstresses.

DOI: 10.61011/PSS.2025.10.62624.278-25

1. Introduction

Heusler alloys belong to the class of functional materials that are promising for use in various kinds of devices based on the observed effect of magneto strain [1–4], magnetocaloric effect [5–8], elastocaloric effect [9–12], etc. In the context of magneto strain properties, single crystalline specimens exhibit strain magnitudes an order of magnitude greater than polycrystalline ones. In Ni-Mn-Ga alloys the irreversible strain may reach nearly 12 % [13,14]. While on a non-textured polycrystalline specimen, these values are less than 1 % [15,16], and in a textured specimen — 2.6 % [17]. The relatively high labor costs of fabrication of single crystals makes scientists to look for ways to increase the functionality of polycrystalline material. At the same time, it is necessary to solve the problem of high thermocyclic brittleness [18,19]. The main approaches to increasing functionality are the formation of a crystallographic texture by the thermomechanical treatment [20–22], or directed crystallization of the melt and the formation of elongated crystals [23,24]. It is optimal to create texture in the material using a thermomechanical treatment, which also allows to increase the mechanical properties of the material. In [25], it was shown that the formation of a bimodal structure in Heusler alloy of Ni-Mn-Ga-Si system leads to a multiple increase in functional fatigue. In functional materials, there is a similar way to reduce thermocyclic brittleness — the formation of a two-phase structure, where the matrix phase carries the functional load, and the secondary phase acts as a damper for internal stresses of phase transformation [26–30]. When transforming the grain structure by deformation, it is necessary to find the influence of both the size of the crystallites and the level of defects and internal stresses on the physical and mechanical properties of the material. This paper presents the results of a study of the effect of internal stresses (microstress) on the dilation properties of Ni-Mn-Ga-Si alloy in a coarse-grained (CG) state and with a bimodal structure.

2. Materials and research methods

$Ni_{56.2}Mn_{18.8}Ga_{23.2}Si_{1.8}$ alloy was fabricated from high-purity Ni, Mn, Ga and Si components by method of arc melting. The technique involves smelting on a water-cooled copper crucible. As a result of melting, large elongated crystallites up to several millimeters in length are formed in the ingot. Transformation of such a structure into a bimodal one by the thermomechanical treatment is not feasible. The transformation of the as-cast structure is performed by vacuum induction remelting in a crucible with low thermal conductivity. As a result, an equiaxed structure with a grain size of about 100 μm is formed. The resulting state is further referred to as the initial state. In a previous study of this alloy by differential scanning calorimetry, it was shown that the characteristic temperatures of the martensitic transformation have the following values: $M_S = 75\,^\circ C$, $M_F = 64\,^\circ C$, $A_S = 73\,^\circ C$ and $A_F = 87\,^\circ C$ for initial state $M_S = 75\,^\circ C$, $M_F = 52\,^\circ C$, $A_S = 58\,^\circ C$ and $A_F = 88\,^\circ C$ for the forged state [31]. In this case, the martensitic transformation is superimposed on the magnetic transformation.

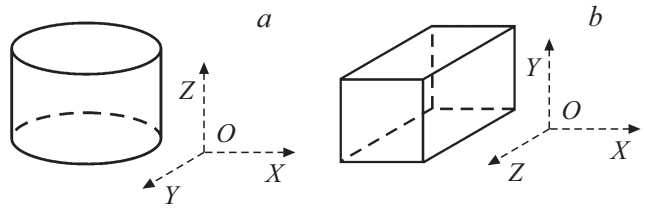

Figure 1. The scheme of the directions of the workpiece in the initial and forged states.

The multi isothermal forging (MIF) is carried out at 700 °C on Schenck-Trebel RMC 100 press system by sequential setting by 35–40 % in $OZ \rightarrow OX \rightarrow OY \rightarrow OX \rightarrow OY \rightarrow OX \rightarrow OY$ directions, where the last 4 passages (upsetting) are made with the specimen tilting along OZ axis (Figure 1). The total true degree of deformation was $e = 3.2$. The alloy billet in its initial state had a cylindrical shape with dimensions $d = 16.3$ mm, $h = 13.3$ mm. As a result of hot forging, the workpiece took the shape of an elongated parallelepiped with dimensions 11.0 mm × 10.7 mm × 23.8 mm.

The analysis of the fine structure parameters of the specimens was carried out at room temperature by X-ray diffraction analysis. The microstructure was studied on a Mira 3 LMH scanning electron microscope (Tescan) in the compositional contrast mode. The curves of the temperature dependence of thermal expansion are recorded on an induction dilatometer. In all cases, the measurement was performed along the long side of the specimens with a size of 7 mm × 1 mm × 1 mm.

3. Results and discussion

3.1. Microstructure

The microstructure was studied in the orientation contrast mode in the plane YOX (Figure 1, *a*) at room temperature, i. e. in the martensitic state of the alloy. The structure of the initial state consists of martensitic colonies occupying the entire volume of grains (Figure 2, *a*). Based on the characteristic change in martensite orientations, the crystallite size can be estimated to be 100–200 μm. It is particularly worth noting that as a result of vacuum induction remelting, the as-cast elongated crystals characteristic of arc smelting are transformed into equiaxed coarse grains. Studies of crystallographic orientations of similarly obtained alloys show that there are no small-angle boundaries in the grain. This suggests that the structure of the initial state is relaxed with a minimum of internal stresses.

The microstructure of the alloy after hot forging is shown in Figure 2, *b, c*. As in the initial state, the study was performed in the plane YOX (Figure 1, *b*). In a deformed workpiece, this is the plane across the stretching axis. The vertical of the pattern is parallel to the compression axis at the final stage of forging. As you can see, the structure is a bimodal structure of a „necklace“ type. The entire volume is occupied by martensitic colonies, by changing the orientations of which it is possible to draw a conclusion about the size of the crystallites. The initial grains of about 100 μm are surrounded by a layer of dynamically recrystallized fine-grained structure. The size of the recrystalline grains makes about 5 μm, and the thickness of layer 20–30 μm (Figure 2, *c*). We have previously shown the possibility of obtaining such a structure by hot forging in Ni-Mn-Ga-Si alloy [32–35]. The formation of „necklace“ is due to the fact that during hot plastic deformation, the density of dislocations increases and at a certain combination of temperature, degree and rate of deformation at the grain boundary, the density reaches a critical threshold, after which the process of dynamic recrystallization begins. With an increase in the true degree of deformation, further nucleation and growth of new grains occur. The grain size in the center of the interlayer and on its periphery is almost the same, which indicates a relatively slow migration of new grain boundaries. In the body of large grains, against the background of martensitic colonies, some blurring of contrast in the body of the twins is visible, indicating the presence of small-angle misorientations. Their presence affects the nature of the twin boundaries, which in the forged state are not rectilinear as in the initial state, but bend slightly throughout its entire length. A general analysis of the alloy structure shows that the large grains are somewhat flattened along the compression axis of the final forging stage. A metallographic grain texture with an extraction coefficient of about 3 is formed by stretching and is oriented along its axis. The orientation of twinning planes in large grains tends to be oriented across the compression axis of the final forging stage. In the inner layer of the fine-grained structure, martensite is oriented chaotically.

3.2. Parameters of the alloy fine structure

The parameters of the fine structure of the alloy were determined at room temperature (martensitic state) by comparative analysis of diffraction patterns. Figure 3 shows diffraction patterns of alloy in its initial and forged states. Decoding of the diffraction patterns showed that, as the initial alloy, it is a mixture of two phases, one of which belongs to a tetragonal (35 % by weight) lattice, and the other to an orthorhombic lattice (65 % by weight). The tetragonal lattice has a symmetry I4/mmm with parameters $a = b = 0.3881$ nm and $c = 0.5963$ nm, and orthorhombic — Pmmm with parameters $a = 0.3719$ nm, $b = 0.4857$ nm and $c = 0.5963$ nm. As a result of hot deformation by forging, the mass ratio of the phase mixture has not changed.

To determine the micro-distortions of the crystal lattice, the broadening and positions of the reflexes were analyzed using the modified Williamson-Hall method. The analysis showed that in the deformed state the level of microdistortions of the crystal lattice is 0.273 %, and in the coarse-

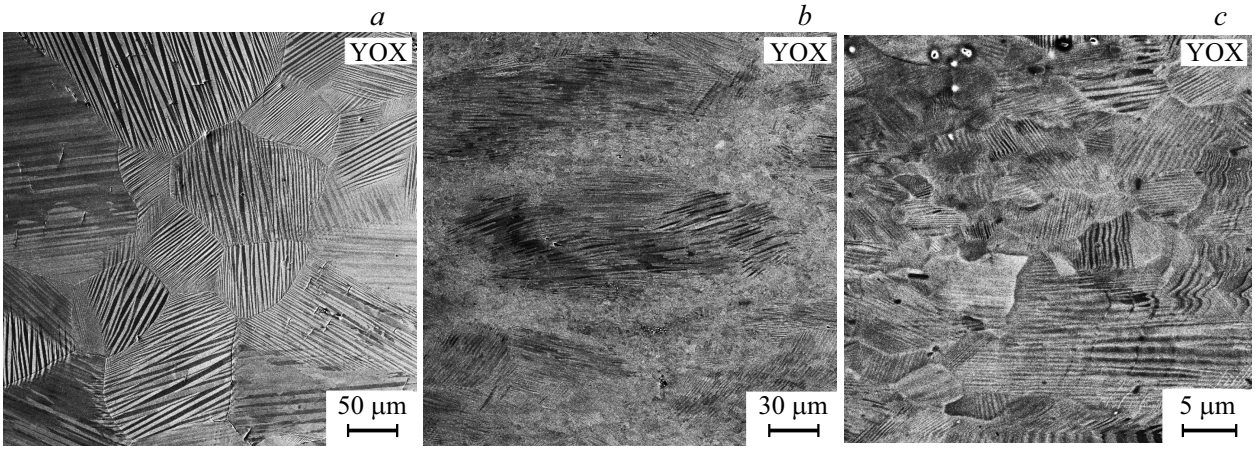

Figure 2. Microstructure of $Ni_{56.2}Mn_{18.8}Ga_{23.2}Si_{1.8}$ alloy in its initial state in plane YOX (a) and forged state in plane YOX (b, c).

grained state it is 0.138 %. The non-zero value of the micro-distortions of the crystal lattice in the initial state is due to the formation of a twin martensitic structure, which, according to electron microscopic studies, has a width of about $1\,\mu$m. As a result of hot deformation by forging, the level of micro-distortions of the crystal lattice increases approximately twofold. Higher amount of micro-distortions of the deformed alloy may be explained by an increase in the density of introduced dislocations as a result of forging.

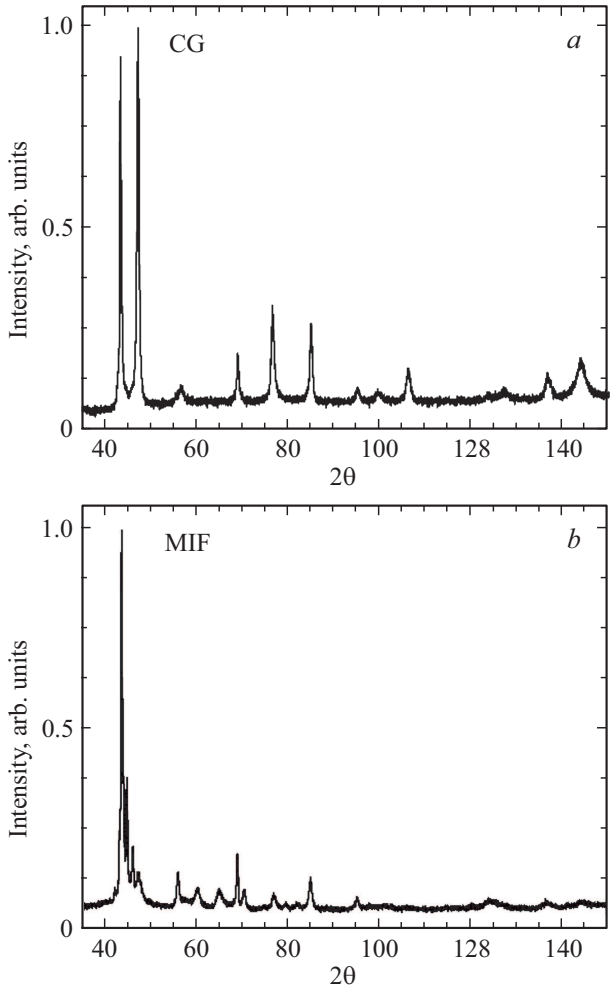

Figure 3. Diffraction pattern of$Ni_{56.2}Mn_{18.8}Ga_{23.2}Si_{1.8}$ alloy in the initial (a) and forged (b) states.

3.3. Dilation of the alloy in various states

The study of the thermal expansion of the alloy was performed in the range of martensitic transformation during heating and cooling of the specimen. Figure 4, *a* shows the dilation curves for the alloy in its initial coarse-grained state. In the process of direct transformation, a barely noticeable reversible abrupt reduction in the length of the specimen is observed. If we draw a straight line parallel to the anharmonic change in length in the austenitic phase, then its intersection with the ordinate axis will show the contribution of the martensitic transformation to the change in length. In this case, the amount of reversible deformation is ~ 0.04 %. Despite the small magnitude of the abrupt change in length during the phase transformation, it is possible to estimate the characteristic temperatures of the martensitic transformation. They are marked with arrows in the drawing. The temperatures differ slightly from the temperatures determined by DSC [31] method. This is due to the fact that in the dilation experiment, the thermocouple is located close to the specimen, while in the DSC experiment it touches the specimen under study. Thus, in the initial state with a equiaxed coarse grain structure a change (close to anharmonic) in the length of the specimen occurs during the martensitic transformation.

The measurement of the dilatation properties of the forged state was performed for specimens cut in two mutually perpendicular directions. The first specimen was cut along the compression axis of final passage during forging (OY, Figure 1, *b*), the second specimen was cut along the stretching axis (OZ, Figure 1, *b*). In the case of both samples, a reversible change in length is observed during the phase transformation. The first specimen, as well as

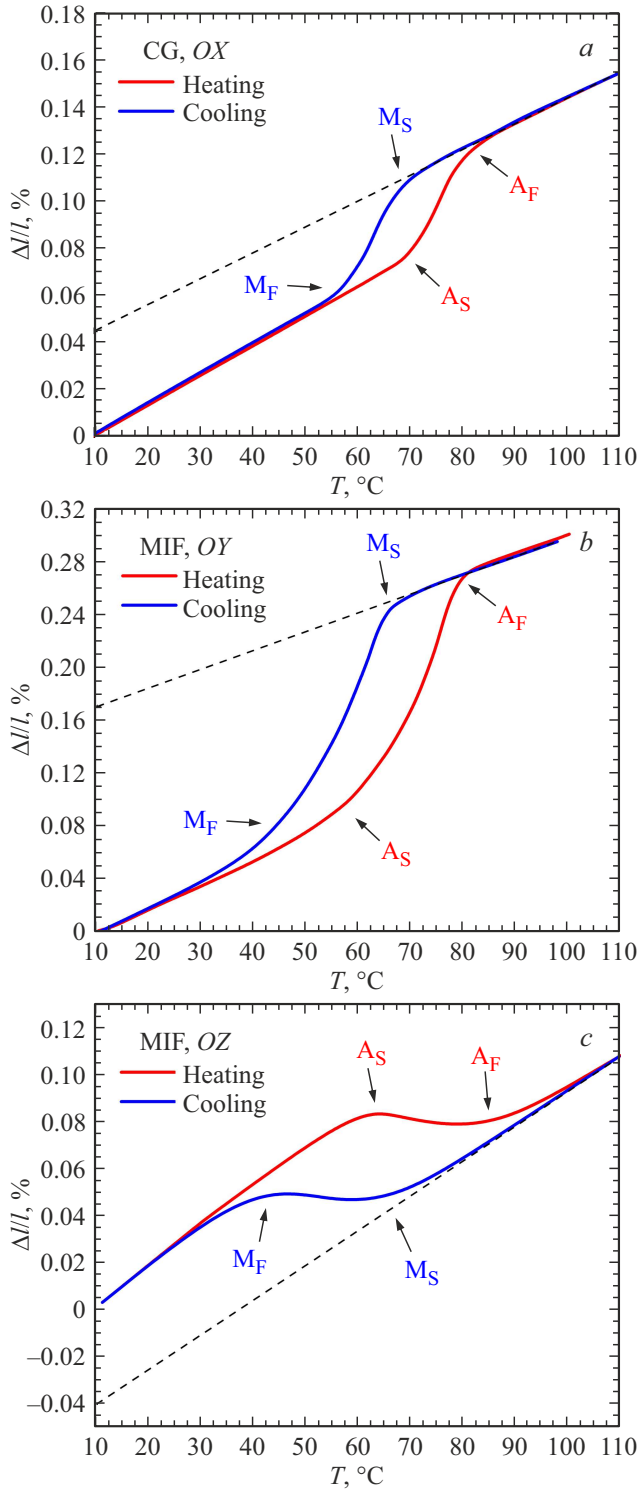

Figure 4. Dilatation curves of the alloy $Ni_{56.2}Mn_{18.8}Ga_{23.2}Si_{1.8}$ in the initial state (*a*), forged state on the specimen, cut along *OY* (*b*) and along *OZ* (*c*).

the specimen in the initial state, demonstrates a downward jump of 0.17 % during the direct martensitic transformation. In the second specimen, the abrupt reduction in length during the direct martensitic transformation is replaced by an abrupt elongation („jumps up“) by 0.05 %. Thus, in the forging state, the alloy in the martensitic transformation region exhibits anisotropy of thermal expansion, which is determined by the direction of the compression axis.

4. Discussion

The anisotropy of thermal expansion of Heusler alloys is a frequently observed phenomenon. Thus, single crystal samples always exhibit anisotropy depending on the direction of measurement (Figure 5) [36–38]. The effect is due to the predominant selection of twinning directions in single crystal specimens. It is shown that the non-directional internal stresses formed during quenching of the sample from the annealing temperature contribute to a sharp decrease in the magnitude of the „jump“. If during thermal treatment the specimen is not subjected to annealing at 500 °C, then the „jump down“ declines from 1.2 % (curve *a*, Figure 5) to 0.4 %.

A polycrystalline specimen, unlike a single crystal, contains grains with different crystallographic orientations. In such a specimen, the predominant direction of the twins should not be formed. And in the process of martensitic transformation, there should be no abrupt change in the length of the specimen. However, there are studies in the literature that show both the presence and absence of abrupt changes in the length of polycrystalline specimens during the martensitic transformation [36,39,40]. Even if an abrupt change in the length of a polycrystalline sample is present during the structural transformation, its magnitude is somewhat less than that of single crystals.

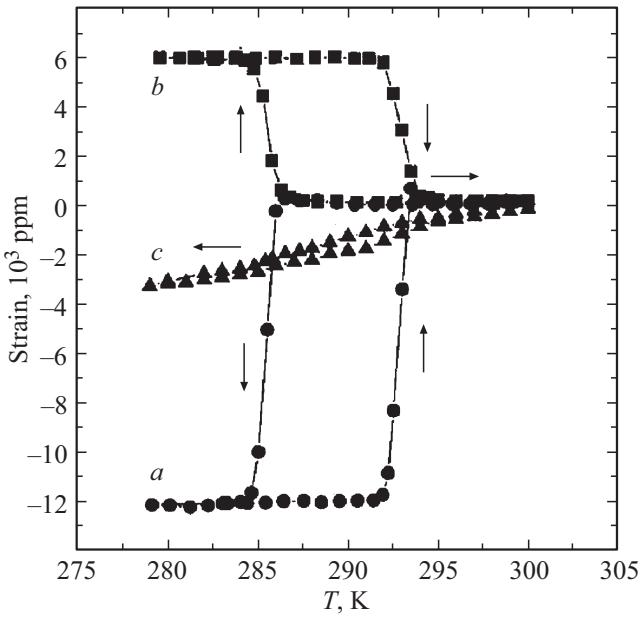

Figure 5. Temperature dependence curves of thermal expansion measured along the crystallographic directions [001] (*a*) and [100] (*b*) of a single-crystal and polycrystal (*c*) for $Ni_{52}Mn_{24}Ga_{24}$ alloy [36].

Earlier, the author showed that the anisotropy of thermal expansion in the region of martensitic transformation in a polycrystalline Heusler alloy specimen is due to the formation of a preferential orientation of martensite [41]. In the as-cast alloy $Ni_{2.08}Mn_{0.96}Ga_{0.96}$, a predominant orientation of transformation twins is observed in the structure of the martensitic phase. If you cut out a specimen with dimensions $7\,mm \times 1\,mm \times 1\,mm$ so that the martensite is predominantly oriented across its long side, the sample shrinks abruptly during the direct martensitic transformation („jumps down"). If you cut the martensite along the long side, then the specimen, on the contrary, lengthens („jumps up"). In this case, the formation of the preferred orientation of martensite was due to the presence of directional internal stresses formed during the crystallization of the melt during the counter-growth of ingot crystals in a deepened water-cooled crucible. To remove internal stresses, high-temperature annealing shall be performed. To select the annealing temperature, it is necessary to know the recrystallization temperature of the alloy. Thus, in the study [42] it was shown that as a result of intense plastic deformation by torsion with a true degree of deformation $e = 6$ of this alloy, annealing at 400 °C already demonstrates the beginning of collective recrystallization. However, at heat treatment temperatures below 400 °C, internal stress relief can only be performed in a material with a high density of defects generated by a very high degree of deformation. In the cast state, the level is clearly lower. Therefore, a higher temperature is chosen to relieve the internal stresses of the as-cast state. Annealing of the as-cast specimen at 650 °C for 2 hours led to relaxation of internal stresses. As a result, in the process of direct martensitic transformation, transformation twins with a chaotic orientation were formed and the abrupt change in the length of the specimen vanished.

In the case of the alloy studied in this work, directional internal stresses are formed by hot forging at 700 °C with a true degree of deformation $e = 3.2$. A comparative analysis of the X-ray diffraction data shows that the level of micro-stress in the relaxed coarse-grained and deformed bimodal structures is different. It should be noted that the studies were made at a room temperature, i. e. in the martensite phase. Therefore, the presence of transformation twins with a diameter of about $1\,\mu m$ contributes to the level of micro-distortions of the lattice. Even in the coarse-grained structure it is non-zero and made 0.138 %. In the forged state, as well as in the martensitic state, it is twice as high and amounted to 0.273 %. As the microstructural analysis data showed, in the coarse-grained state, a chaotic orientation of the transformation twins is indeed observed, while in the forged state, some of their preferential orientation is observed. When cutting the specimen with the long side along the compression axis at the final forging stage, the twins in its structure are mainly oriented along the length. And such specimen demonstrates a „jump down". The specimen, cut in the perpendicular direction and along the stretching axis, demonstrates an „upward jump". The direction of compression forms the predominant orientation of internal stresses. This leads to a decrease in the directions sampling during the twinning of the structure in the process of direct martensitic transformation. The internal stresses may be enhanced by two ways. Either by increasing the degree of deformation, or by reducing the deformation temperature at the last stage of forging. The continuation of this line of research involves the implementation of both methods.

Thus, the paper establishes the main patterns of the influence of internal stresses (micro-stress) on the anisotropy of the thermal expansion of the alloy specimen of the system during martensitic transformation. It is shown that the compression axis at the final stage forms a preferential orientation of internal stresses, which leads to a preferential orientation of the martensite and, as a result, to anisotropy of changes in the geometry of the specimen during phase transformation.

5. Conclusion

In the alloy $Ni_{56.2}Mn_{18.8}Ga_{23.2}Si_{1.8}$, as a result of arc melting and subsequent induction remelting in a quartz crucible, the as-cast structure with elongated crystals was transformed into an equiaxial coarse-grained structure with a crystallite size of about $100\,\mu m$. As a result of hot forging at 700 °C ($e = 3.2$), a bimodal structure of „necklace" type was formed, where the initial large grains are surrounded by a layer of dynamically recrystallized fine-grained structure. In such a structure, the level of micro-distortions of the lattice exceeds that of the initial alloy by about two times. In the bimodal structure, the predominant orientation of the transformation twins and the anisotropy of thermal expansion in the region of the martensitic transformation are formed.

Funding

The present work was accomplished according to the state assignment of the Institute for metals superplasticity problems RAS. The studies were carried out on the facilities of shared services center of the Institute for Metals Superplasticity Problems of Russian Academy of Sciences „Structural and Physical-Mechanical Studies of Materials".

Conflict of interest

The author declares that he has no conflict of interest.

References

[1] S. Tavares, K. Yang, M.A. Meyers. Progress in Materials Science **132**, 101017 (2023).
[2] V. Chernenko. Magnetostrictive Ni-Mn-based Heusler alloys. Encyclopedia of Smart Materials. Elsevier (2022). P. 160–176.
[3] Q. Yang, X. Wu, Y. Gu, Y. Shi. J. Alloys Compd. **1035**, 181559 (2025).

[4] S.Y. Yu, A.J. Gu, S.S. Kang, S.J. Hu, Z.C. Li, S.T. Ye, H.H. Li, J.J. Sun, R.R. Hao. J. Alloys Compd. **681**, 1-5 (2016).
[5] K. Ahn. J. Alloys Compd. **978**, 173378 (2024).
[6] V.V. Sokolovsky, M.A. Zagrebin, V.D. Buchelnikov, V.V. Marchenkov. FMM. **124**, *11*, 1019-1024 (2023). (in Russian).
[7] V.V. Sokolovskiy, A.P. Kamantsev, V.D. Buchelnikov, V.V. Marchenkov. Physics of Metals and Metallography **125**, *14*, 1805-1813 (2024).
[8] V.I. Valkov, A.V. Golovchan, I.F. Gribanov, O.E. Kovalev, V.I. Mityuk. FTT **66**, *6*, 988-999 (2024). (in Russian).
[9] Y. Shen, W. Sun, Z.Y. Wei, Q. Shen, Y.F. Zhang, J. Liu. Scripta Materialia **163**, 14-18 (2019).
[10] Z. Li, Z. Li, Y. Lu, X. Lu, L. Zuo. Journal of Materials Science and Technology **117**, 167-173 (2022).
[11] C. Huang, Y. Wang, Z. Tang, X. Liao, S. Yang, X. Song. J. Alloys Compd. **630**, 244-249 (2015).
[12] J. Yang, H. Wang, Z. Li, N. Zou, H. Yan, B. Yang, L. Zuo. Acta Materialia **263**, 119546 (2024).
[13] R. Chulist, E. Pagounis, P. Czaja, N. Schell, H. Brokmeier. Adv. Eng. Mater. **23**, 2100131 (2021).
[14] A. Sozinov, N. Lanska, A. Soroka, W. Zou. Appl. Phys. Lett. **102**, *2*, 021902 (2013).
[15] Z. Zhou, P. Wu, G. Ma, B. Yang, Z. Li, T. Zhou, D. Wang, Y. Du. J. Alloys Compd. **792**, 399–404 (2019).
[16] S.Y. Yu, A.J. Gu, S.S. Kang, S.J. Hu, Z.C. Li, S.T. Ye, H.H. Li, J.J. Sun, R.R. Hao. J. Alloys Compd. **681**, 1–5 (2016).
[17] A.A. Mendonca, J.F. Jurado, S.J. Stuard, L.E.L. Silva, G.G. Eslava, L.F. Cohen, L. Ghivelder, A.M. Gomes. J. Alloys Compd. **738**, 509–514 (2018).
[18] W. Everhart, J. Newkirk. Heliyon **5**, *5*, e01578 (2019).
[19] Q. Xia, X. Tian, W. Zhao, C. Tan, K. Zhang. Mater. Today Commun. **38**, 108089 (2024).
[20] R. Chulist, W. Skrotzki, C.-G. Oertel, A. Bohm, H.-G. Brokmeier, T. Lippmann. Int. J. Mat. Research. **103**, *5*, 575-579 (2012).
[21] L. Wei, X. Zhang, M. Qian, X. Cui, L. Geng, J. Sun, L.V. Panina, H.-X. Peng. Mater. Design. **112**, *339-344* (2016).
[22] R. Chulist, A. Bohm, E. Rybacki, T. Lippmann, C.G. Oertel, W. Skrotzki. Mater. Sci. Forum **702–703**, 169–172 (2011).
[23] L. Wei, X. Zhang, J. Liu, L. Geng. AIP Advances **8**, *5*, 055312 (2018).
[24] D. Li, Z. Li, J. Yang, Z. Li, B. Yang, H. Yan, D. Wang, L. Hou, X. Li, Y. Zhang, C. Esling, X. Zhao, L. Zuo. Scripta Materialia **163**, 116-120 (2019).
[25] I.I. Musabirov, I.M. Safarov, R.M. Galeyev, D.D. Afonichev, R.Y. Gaifullin, V.S. Kalashnikov, E.T. Dilmieva, V.V. Koledov, S.V. Taskaev, R.R. Mulyukov. Trans. Indian Inst. Met. **74**, 2481–2489 (2021).
[26] I.D. Kurlevskaya, E.Y. Panchenko, A.B. Tokhmetova, E.I. Yanushonite, A.S. Eftifeeva, N.Yu. Surikov, E.E. Timofeeva, Yu.I. Chumlyakov. Phys. Mesomech. **27**, 398–408 (2024).
[27] E.E. Timofeeva, E.Y. Panchenko, M.C. Dmitrienko, E.I. Yanushonite, I.D. Fatkullin, Yu.I. Chumlyakov. Pis'ma v ZhTF **51**, *11*, 46-51 (2025). (in Russian).
[28] Z. Lin, X. Wang, F. Zhu, B. Li, S. Bi. Mater. Today Commun. **47**, 112952 (2025).
[29] J. Meng, L. Xie, Q. Yu, J. Wang, C. Jiang. Acta Materialia **263**, 119469 (2024).
[30] Q. Zhai, F. Bu, Y. Cheng, J. Zhang, Y. He. J. Magn. Magn. Mater. **629**, 173246 (2025).
[31] R.Yu. Gayfullin, A.B. Hajiyev, A.M. Aliev, S.V. Taskaev, I.I. Musabirov. Radiotekhnika i elektronika, **68**, *4*, 346-352 (2023). (in Russian).
[32] I.I. Musabirov, I.M. Safarov, R.M. Galeev, R.A. Gaisin, V.V. Koledov, R.R. Mulyukov. FTT **60**, *6*, 1051-1057 (2018). (in Russian).
[33] I.I. Musabirov, I.M. Safarov, R.M. Galeev, D.D. Afonichev, R.Yu. Gayfullin, V.V. Koledov, S.V. Taskaev, R.R. Mulyukov. Chelyabinsk physical and mathematical magazine **5**, *4-2*, 601-611 (2020).
[34] I.I. Musabirov, R.Y. Gaifullin, A.B. Gadjiev, A.M. Aliev, E.T. Dilmieva, S. Krämer, Yu.S. Koshkid'ko. J. Magn. Magn. Mater. **594**, 171892 (2024).
[35] I.I. Musabirov, I.M. Safarov, R.M. Galeev, D.D. Afonichev, V.V. Koledov, A.I. Rudskoy, R.R. Mulyukov. Fizika i mekhanika materialov **33**, *1*, 124-136 (2017). (in Russian).
[36] W.H. Wang, G.H. Wu, J.L. Chen, C.H. Yu, S.X. Gao, W.S. Zhan, Z. Wang, Z.Y. Gao, Y.F. Zheng, L.C. Zhao. Appl. Phys. Lett. **77**, *20*, 3245–3247 (2000).
[37] F. Xiong, Y. Liu, E. Pagounis. J. Magn. Magn. Mater. **285**, 410-416 (2005).
[38] T. Liang, C. Jiang, H. Xu. Mater. Scien. Engineer. A. **402**, 5-8 (2005).
[39] A.N. Vasilev, E.I. Estrin, V.V. Khovailo, A.D. Bozhko, R.A. Ischuk, M. Matsumoto, T. Takagi, J. Tani. Int. J. Appl. Electromagn. Mechan. **12**, 35-40 (2000).
[40] Yu.V. Kaletina, E.G. Gerasimov, V.A. Kazantsev, A.Yu. Kaletina. FTT **59**, *10*, 1978-1983 (2017).
[41] I.I. Musabirov, H.Ya. Mulyukov, V.V. Koledov, V.G. Shavrov. ZHTF, 108-111 (2011). (in Russian).
[42] I.I. Musabirov, I.M. Safarov, R.R. Mulyukov, I.Z. Sharipov, V.V. Koledov. Letters on Materials **4**, *4(16)*, 265-268 (2014).

Translated by T.Zorina